Available online at www.sciencedirect.com

ScienceDirect

European Journal of Protistology 87 (2023) 125940

European Journal of PROTISTOLOGY

www.elsevier.com/locate/ejop

Morphology and molecular phylogeny of the benthic dinoflagellates (Dinophyceae, Peridiniales) *Amphidiniopsis crumena* n. sp. and *Amphidiniopsis nileribanjensis* n. sp.

Aika Yamaguchi [a,*], Mona Hoppenrath [b], Shauna Murray [c], Anna Liza Kretzschmar [c,d], Takeo Horiguchi [a], Kevin C. Wakeman [e]

[a] *Faculty of Science, Hokkaido University, North 10, West 8, Sapporo 060-0810 Japan*
[b] *Senckenberg am Meer, German Centre for Marine Biodiversity Research, Südstrand 44, D-26382 Wilhelmshaven, Germany*
[c] *University of Technology Sydney, School of Life Sciences, 15 Broadway, Ultimo, NSW 2007, Australia*
[d] *Garvan-Weizmann Centre for Cellular Genomics, Garvan Institute of Medical Research, Sydney, NSW 2010, Australia*
[e] *Institute for International Collaboration, Hokkaido University, Sapporo 060-0808 Japan*

Received 7 September 2022; revised 1 November 2022; accepted in revised form 2 November 2022; available online 7 November 2022

Abstract

Amphidiniopsis is a benthic, heterotrophic and thecate dinoflagellate genus that has a smaller epitheca and larger hypotheca. The genus contains 24 described species, but is considered to be polyphyletic based on morphological characters and molecular phylogenetics. In this study, two new species were discovered from two distant sampling localities, *Amphidiniopsis crumena* sp. nov. from Japan, and *Amphidiniopsis nileribanjensis* sp. nov., from Australia. These species have a uniquely shaped, additional second postcingular plate. Both species are dorsoventrally flattened, an apical hook is present, and have six postcingular plates. The plate formula is: APC 4′ 3a 7″ ?C 4?S 6‴ 2⁗. The cells of these species were examined with LM and SEM, and molecular phylogenic analyses were performed using 18S and 28S rDNA. These species are distinguished by the presence of spines on the hypotheca and touching of the sixth postcingular plate and the anterior sulcal plate. Their shape and disposition of several thecal plates also differ. Molecular phylogenetic analyses showed that the two new species formed a monophyletic clade and did not belong to any morphogroup proposed by previous studies. Considering the morphological features and the molecular phylogenetic results, a new morphogroup is proposed, *Amphidiniopsis* morphogroup VI ('*crumena* group').

Keywords: Biodiversity; Heterotrophic protist; Microscopy; Morphogroup; Taxonomy

Introduction

Dinoflagellates inhabit a wide variety of environments and employ a diverse set of life strategies, living as marine and freshwater plankton, within marine sand, on the macroalgae surface as epiphytes, and in the tissues of other eukaryotes. Around half of all dinoflagellates are photosynthetic, while the other half is heterotrophic; some also live as mixotrophic and obligate symbionts/parasites (Fensome et al. 1993).

*Corresponding author at: Faculty of Science, Hokkaido University, North 10, West 8, Sapporo 060-0810, Japan.
E-mail address: aikay1120@yahoo.co.jp (A. Yamaguchi).

https://doi.org/10.1016/j.ejop.2022.125940
0932-4739/

The genus *Amphidiniopsis* is a benthic (sand-dwelling), heterotrophic and thecate dinoflagellate that is defined by its smaller epitheca and relatively larger hypotheca (Hoppenrath et al. 2014). This benthic dinoflagellate genus is one of the largest and currently encompasses 24 described species (Hoppenrath et al. 2014; Reñé et al. 2020; Selina and Morozova 2016). It was established by Wołoszy ska in 1928 with the type species *A. kofoidii* Wołoszy ska, based on observations by light microscopy (LM) documented as detailed line drawings (Wołoszy ska 1928). The first observation by scanning electron microscopy (SEM) for *Amphidiniopsis* spp. was performed by Dodge and Lewis (1986) and they emended the plate formula of the original description of *A. kofoidii*. After the 20th century, new species of *Ampidiniopsis* were described through both LM and SEM observations (Hoppenrath 2000; Hoppenrath et al. 2009, 2012, 2014; Murray and Patterson 2002; Reñé et al. 2020; Selina and Hoppenrath 2013; Selina and Morozova 2016; Toriumi et al. 2002; Yoshimatsu et al. 2000). Since species of the genus have various morphologies, three major subgroups were proposed to subdivide the genus (Hoppenrath et al. 2012, 2014). These three subgroups, namely Group 1, 2 and 3, were distinguished by the general cell shape, the features of the cingulum and sulcus, the presence or absence of the apical hook, the number of anterior intercalary plates, and the position of the second intercalary plate (Hoppenrath et al. 2012, 2014). Some studies performed molecular phylogenetic analyses using 18S ribosomal DNA (rDNA) and 28S rDNA sequences to infer phylogenetic positions within the genus and among other dinoflagellate groups (Gómez et al. 2011; Hoppenrath et al. 2012; Reñé et al. 2020; Yamaguchi et al. 2016). The resulting 18S and 28S rDNA phylogenies showed that most *Amphidiniopsis* species, the benthic *Herdmania litoralis* Dodge, and planktonic members within the *Protoperidinium* "*monovelum*" formed a single, well-supported clade. The only exception to this was *A*. cf. *arenaria* Hoppenrath that clusters outside this clade. Within this clade, some subclades contained both representatives of *Amphidiniopsis* and the *Protoperidinium* "*monovelum*" section. It was suggested that the sand-dwelling *Amphidiniopsis* is not monophyletic and its taxonomy needs to be reconsidered (Yamaguchi et al. 2016). Reñé et al. (2020) described three new species of *Amphidiniopsis* and performed phylogenetic analyses using 18S rDNA and 28S rDNA sequences. Their phylogenetic reconstructions also suggested the genus was not monophyletic and contained at least four phylogenetic subgroups. They revised the morphogroups of the *Amphidiniopsis* genus complex from Hoppenrath et al. (2014), namely group I ('*kofoidii* group'), group II ('*hirsuta* group'), group III ('*uroensis* group'), group IIIa ('*cristata* group'), group IV ('*rotundata* group') and group V ('*Herdmania* group') (Reñé et al. 2020). To this end, it is important to collect more information of the species of the *Amphidiniopsis* genus complex to revise its taxonomic system presented by these morphogroups.

Two new species belonging to the *Amphidiniopsis* genus complex with a unique shape of a thecal plate were collected from two distant sampling localities in Japan and Australia. The cells of these new species were examined with LM and SEM, and their phylogenetic position was inferred using 18S rDNA and 28S rDNA based on single-cell PCR.

Material and methods

Sampling

In Japan, the sand samples were collected at a surface of tidal flat in Onna Village, Okinawa (26°28′57.05″ N, 127° 50′ 44.49″ E) in April 2017 and Maiko, Kobe, Hyogo Prefecture (34°37′38.58″N, 135°02′ 23.09″E) on 26th June 2017 by scooping with a metal spoon. The sand samples were inoculated in 0.126 g/L (powder) Daigo′s IMK culture medium (Nihon Pharmaceutial Co., Ltd., Tokyo, Japan) in a plastic cup and maintained at 20 °C in a 16 h:8h light/dark cycle for two - three weeks.

Australian samples were collected at Cable Beach, Broome (17.9319° S, 122.2081° E), in the tropical north of Western Australia, in May 2011. Samples were collected from the first 0.5 cm of sediment at low tide using a flat spoon (Murray and Patterson 2002). Dinoflagellates were separated from the sand by extraction through a fine filter (mesh size 55 μm) using the melting seawater-ice method (Hoppenrath et al. 2014; Uhlig 1964).

Isolation and light microscopical observation

Single live cells of *Amphidiniopsis crumena* were isolated and washed several times in serial drops of 0.22 μm filtered seawater by micropipetting, using a ZEISS Primovert microscope (Zeiss, Jena, Germany). Cells were transferred to a glass slide with a vinyl tape frame (Horiguchi et al. 2000) and sealed with a cover glass. Each cell was observed using a BX-50 compound microscope with Nomarski optics (Olympus, Tokyo, Japan) equipped with an EOS Kiss X8i digital camera (Canon, Tokyo, Japan). Single live cells of *Amphidiniopsis nileribanjensis* were isolated by micropipetting and observed using a Leica DMIL inverted microscope (Leica Microsystems GmbH, Wetzlar, Germany) equipped with a Leica DFC290 digital camera.

Single cell isolation and DNA extraction for PCR

In Japan, each photographed cell was transferred to a PCR tube containing 10 μl of Quick Extract FFPE DNA

Extraction Solution (Epicentre, Madison, WI, USA) and incubated for 1 h at 56 °C, then for 2 min at 98 °C. The resulting extract was used as a DNA template for subsequent PCR amplification. For Australian samples, single isolated cells were identified via light microscopy and frozen in up to 10 µl of 0.22 µm filtered sea water and stored at −80 °C until processing.

Scanning electron microscopy (SEM)

Individual cells were isolated and placed in a small container covered on one side with a 10 µm plankton net or a 5 µm polycarbonate membrane filter (Corning Separations, Acton, MA) containing acidic 1% Lugol's Solution in culture medium. They were washed three times in distilled water and dehydrated through a graded series of ethanol (50%, 70%, 80%, 90%, 100%) for 5 mins each step. Samples were critical point dried with CO_2, sputter-coated with 5 nm gold and observed using a Hitachi 4700 Electron Microscope (Hitachi, Tokyo, Japan).

For the Australian samples, mixed samples of extracted dinoflagellates were rinsed in sterile seawater and fixed with Lugol's iodide for ∼4 weeks, were filter-mounted, rinsed with distilled water and dehydrated with 30, 50 and 70% ethanol followed by dimethoxypropane. The filters were critical point dried or air-dried, before being sputter coated with gold or gold/palladium. Samples were analysed on a Zeiss Ultra Plus Field Emission Scanning Electron Microscope (FESEM) at the University of Sydney (Australian Centre for Microscopy and Microanalysis) at 5–15 kV.

Single-cell polymerase chain reaction (SC-PCR) and sequencing

The initial PCR was performed using a total volume of 25 µl with EconoTaq 2X Master Mix (error rate 1 per 20,000–40,000) (Lucigen, Middleton, WI, USA) following the manufacture's protocols. Nearly the entire 18S rRNA gene and the part of the 28S rRNA gene were amplified using the sets of universal eukaryote primers: (SR1: 5′-TACCTGGTTGATCCTGCCAG-3′ and SR12: 5′-CCTTCCGCAGGTTCACCTAC-3′) and (25F1: 5′-CCGCTGAATTTAAGCATAT-3′ and LSU R2: 5′-ATTCGGCAGGTGAGTTGTTAC-3′) (Yamaguchi et al. 2006). The PCR protocol had an initial denaturation stage at 94 °C for 2 min; 35 cycles of denaturation at 94 °C for 30 s, annealing at 55 °C for 30 s, and extension at 72 °C for 2 min; and final extension at 72 °C for 7 min. The first PCR product was used as a DNA template for the second PCR. The second PCR was performed where the following combinations of primer pairs were used separately: SR1b (5′-GATCCTGCCAGTAGTCATATGCTT-3′) and SR5TAK (5′-ACTACGAGCTTTTTAACYGC-3′), SR4 (5′-AGGGCAAGTCTGGTGCCAG-3′) and SR9p (5′-AACTAAGAACRGCCATGCAC-3′), SR8TAK (5′-GGATTGACAGATTGAKAGCT-3′) and SR12, 25F1 and 25R1 (5′-CTTGGTCCGTGTTTCAAGAC-3′), LSU D3A (5′-GACCCGTCTTGAAACACGGA-3′) and LSU R2 (Takano and Horiguchi 2004; Yamaguchi et al. 2006). These combinations of primer-sets cover almost entire region of 18S rDNA and D1-D3 region of 28S rDNA. The PCR protocol had an initial denaturation stage at 94 °C for 2 min; 25 cycles of denaturation at 94 °C for 30 s, annealing at 50 °C for 30 s for 18S rDNA and 48 °C for 28S rDNA, and extension at 72 °C for 45 s; and final extension at 72 °C for 7 min. Amplified DNA fragments corresponding to the expected size were purified by QIAquick PCR Purification Kit (QIAGEN, Hilden, Germany). The cleaned PCR products were sequenced directly by Fasmac sequencing service (Fasmac, Kanagawa, Japan). New sequences have been deposited in DDBJ/EMBL/GenBank under the accession numbers (LC333939–LC333942, LC340364–LC340372).

For the Australian samples, the first round of PCR reactions were set up as follows and directly added to the frozen sample: 2 µl 5x Advantage GC2 polymerase Mix, 10 µl GC melt and 20 µl 5x Advantage GC2 buffer by Clontech (Takara, CA, USA) as well as 10 µM of each deoxynucleotide, and 10 µM of each primer: D1R-F (5′-ACCCGCTGAATTTAAGCATA-3′), D3B (5′-TCGGAGGGAACCAGCTACTA-3′), 18ScomF1 (5′-GCTTGTCTCAAAGATTAAGCCATGC-3′), 18ScomR1 (5′-CACCTACGGAAACCTTGTTACGAC-3′) (Nunn et al. 1996; Scholin et al. 1994; Zhang et al. 2005). Reaction volume was then made up to a total of 100 µl with sterile MilliQ water, depending on amount of sea water present. PCR cycling was initiated with 94 °C for 5 min; followed by 30 cycles of denaturing at 94 °C for 30 s, annealing at 55 °C for 30 s, and extension at 68 °C for 2 min; with a final extension at 68 °C for 3 min. In the second round of PCR, four reactions were set up using the first round of PCR as a template, with the following primer combinations: 18ScomF1 & Dino18SR1 (5′-GAGCCAGATRCDCACCCA-3′); G10F (5′-TGGAGGGCAAGTCTGGTG-3′) & G18R (5′-GCATCACAGACCTGTTATTG-3′); Dino18SF2 (5′-ATTAATAGGGATAGTTGGGGGC-3′) & 18ScomR1; and D1R-F & D3B (Litaker et al. 2005; Nishimura et al. 2013; Nunn et al. 1996; Scholin et al. 1994; Zhang et al. 2005). Reactions were set up with 0.25 µl 5x Advantage GC2 polymerase Mix, 2.5 µl GC melt and 5 µl 5x Advantage GC2 buffer by Clontech (Takara, CA, USA) as well as 10 µM of each deoxy-nucleotide, 10 µM per primer, 0.5 µl reaction template, made up to a final volume of 25 µl with sterile MilliQ water. PCR cycling conditions were the same as in the first round of PCR. The secondary round PCR product was visualized on a 2% agarose gel run at 70 V for 2 hr. Bands were identified in comparison to a positive *Gambierdiscus pacificus* M.Chinain et M. Faust genomic DNA control and extracted as per protocol using the Zymogen (CA, USA) Gel Recovery kit. Sanger sequencing was performed by Macrogen Inc (Seoul, Korea). The new sequence

has been deposited in DDBJ/EMBL/GenBank under the accession numbers (LC719582).

Sequence alignments and phylogenetic analyses

For phylogenetic analyses, the acquired sequences were aligned with the selected taxa based on the dataset from Yamaguchi et al. (2016) using Mesquite 3.6 (Maddison and Maddison 2015) and MUSCLE (Edgar 2004; https://www.ebi.ac.uk/Tools/msa/muscle/), with the default settings. The alignment was trimmed with Gblocks with less stringent selection options; allow smaller final blocks and allow gap positions within the final blocks (Castresana 2000; Talavera and Castresana 2007). The final alignments of the 18S rDNA and 28S rDNA datasets consisted of 86 taxa and 1,673 sites and 82 taxa and 1,109 sites, respectively. The apicomplexan *Neospora caninum* Dubey, Carpenter, Speer, Topper et Uggela was used as the outgroup for both datasets. Phylogenetic trees were constructed using maximum likelihood (ML) and Bayesian analysis. The best-fit models for each dataset were selected using IQ-TREE under AICc (Trifinopoulos et al. 2016). Maximum-likelihood (ML) analyses on the datasets were run with IQ-TREE using GTR + F + R5, as the model of evolution for both the 18S rDNA and 28S rDNA. Each analysis ran for 500 bootstrap pseudoreplicates.

All Bayesian analyses were performed using the program MrBayes 3.2.5 (Ronquist and Huelsenbeck 2003). The program was set to operate with GTR + F + R5 and GTR + F + R4 for 18S rDNA and 28 rDNA analyses, and four Monte Carlo Markov Chains (MCMC) starting from a random tree. A total of 3,000,000 and 1,000,000 runs were completed for 18S rDNA and 28S rDNA datasets, respectively. Generations were calculated with trees sampled every 100 generations and the first 7,500 and 2,500 trees in each run were discarded as burn-in. When the standard deviation of split frequencies fell below 0.01, the program was set to terminate. Posterior probabilities correspond to the frequency at which a given node was found in the post-burn-in trees.

Results

Species descriptions

Amphidiniopsis crumena A.Yamag., T.Horiguchi et Wakeman sp. nov.

Figs. 1–3.

Description: Cells rounded in ventral view, slightly flattened dorsoventrally, slightly elongated (Figs. 1–2), 23.2–31.2 μm long (n = 13), and 20.5–30.0 μm wide (premedian) (n = 13). Apical hook pointing to the left cell side (Fig. 1l, Fig. 2a). Irregular hypothecal and antapical spines (Fig. 1h, j, l). Serrated left sulcal list (Fig. 1j). No chloroplast, eyespot or recognizable food particles, but several orange lipide drops in the cytoplasm (Fig. 1). Two pusules are seen, one is in the episome and another is in the hyposome (Fig. 1h, l, p). Nucleus in the hyposome (Fig. 1m).

Thecal plate formula: APC 4′ 3a 7″ ?C 4S 6‴ 2⁗. Apical Pore Complex (APC) with cover plate (Pi) covering the oval apical pore and outer pore plate (Po) surrounding the apical pore (Fig. 3b). Canal plate (X) not observed. First apical plate (1′) elongated shifted left laterally (Fig. 2c). Third apical plate (3′) largest apical plate located dorsal (Fig. 1c, Fig. 2c–d). The ridge of the 3′ plate formed an apical hook pointing the left side of the cell (Fig. 2c–d, Fig. 3b). Fourth apical plate (4′) in ventral right position (Fig. 2a–c). Small pentagonal first anterior intercalary plate 1a in left lateral position (Fig. 2b–c, Fig. 3a). Second anterior intercalary plate 2a in left lateral position, hexagonal, long and narrow (Fig. 2c, Fig. 3a). Third anterior intercalary plate 3a also hexagonal and wide, occupies the middle part of the dorsal epitheca (Fig. 2d). First precingular plate (1″) narrow and running vertically (Fig. 2a–c). Very small, pentagonal second precingular plate (2″) (Fig. 2b–c, Fig. 3a). Very long and narrow, four-sided, third precingular plate (3″) in left lateral position (Fig. 2c–d, Fig. 3a). Fourth (4″) and fifth (5″) precingular plate narrow elongated, dorsal (Fig. 2d, Fig. 3d). Larger pentagonal sixth precingular plate (6″) in right lateral position (Fig. 3c–d). Ventral seventh precingular plate (7″) pentagonal (Fig. 2a–c, Fig. 3c, f).

Cingulum wide, ascending, completely encircling the cell (Fig. 1f, j, Fig. 2a–c). As cingular plate contacts were not clearly visible the number of plates is uncertain. Wide sulcus consisting of non-recessed and recessed plates (forming the longitudinal furrow). Non-depressed anterior sulcal plate (Sa) between right and left edge of the cingulum (Fig. 2a–b). Non-depressed, large right sulcal plate (Sd) with well-developed wing-like left list positioned mid ventrally (Fig. 2a). Depressed, elongated left sulcal plate (Ss) connected to the left cingulum origin (Fig. 2b). Posterior sulcal plate (Sp) positioned antapically, below Sd and Ss. (Fig. 2a, Fig. 3f). We could not observe the flagellar pores by both LM and SEM observations. Very short postcingular list formed by the postcingular plates, except for plate 2‴ for which this list runs around the plate (formed by the connecting plates 1‴ and 3‴) (Fig. 2a–b). First postcingular plate (1‴) elongated with serrated left side contacting with the first antapical plate (1⁗) and serrated right side forming the left sulcal list (Fig. 2a–b). Striking, small second postcingular plate (2‴) with unique pocket-like shape that is curved except for the straight suture that touches the cingulum in ventral position (Fig. 1a, f, k, Fig. 2a–b). Fourth postcingular plate (4‴) symmetrical, pentagonal (Fig. 2d, Fig. 3d) and positioned dorsal. Third (3‴) and fifth (5‴) postcingular plates in lateral position (Fig. 2b, d, Fig. 3a, d). Large sixth (6‴) postcingular plate covering the right ventral hypotheca part (Fig. 2a, Fig. 3f). Two antapical plates (1⁗, 2⁗) with irregular spiny lists, showed their similar size on the dorsal view of the hypotheca (Fig. 1h, l, Fig. 2a–b, d Fig. 3d, f, Fig. 8a–b).

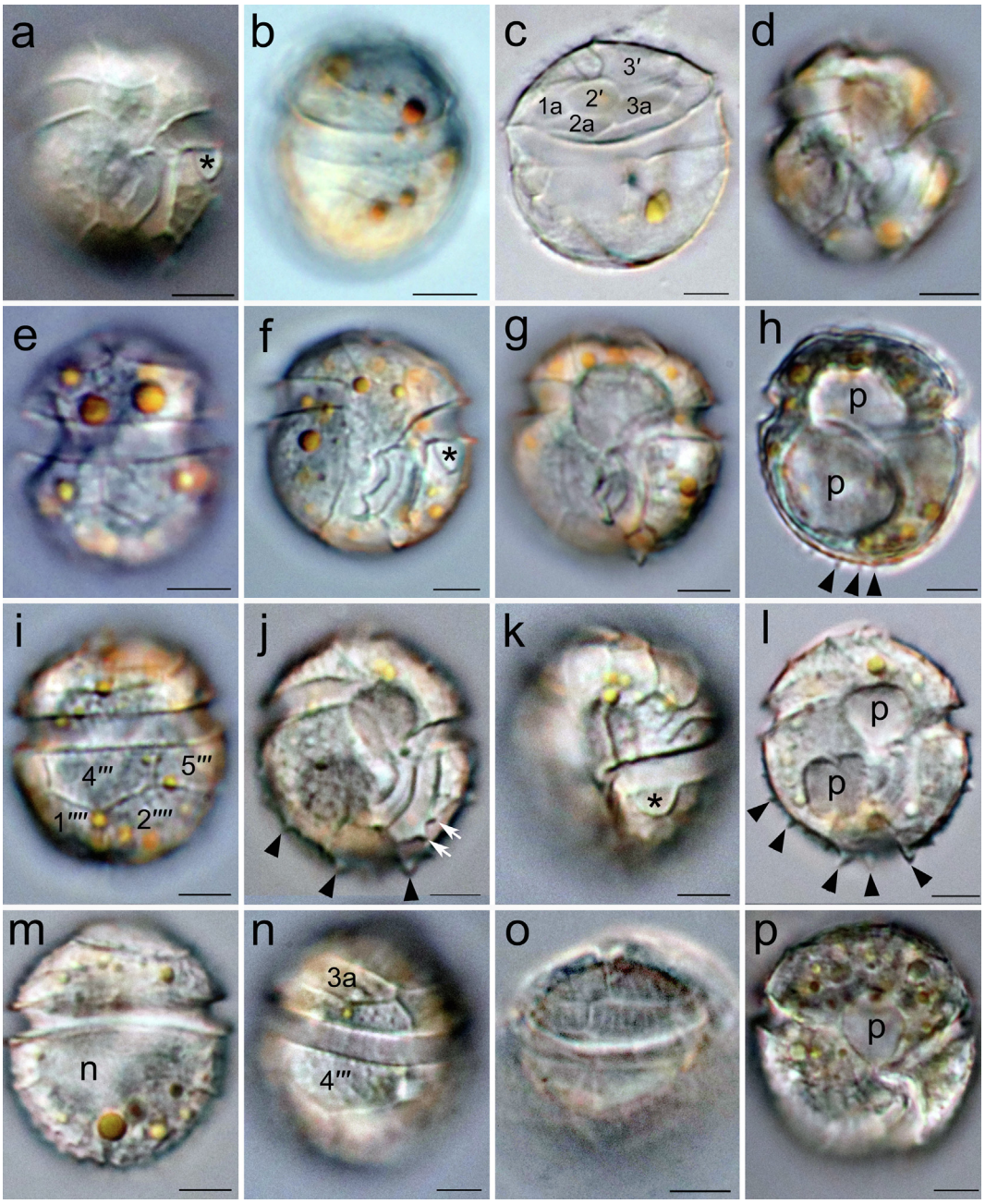

Fig. 1. Light micrographs of the single-cells of *Amphidiniopsis crumena* from Okinawa, Japan and Kobe, Japan used for rDNA sequencing. Scale bars = 5 μm. **a.** Ventral view of *A. crumena* individual number A1 showing the second postcingular plate (2‴) that has the round curve (asterisk). **b–c.** *A. crumena* individual number A2. **b.** Dorsal view. **c.** The crashed empty theca showing the apical plates (2′, 3′) and the first to the third anterior intercalary plates 1a-3a. **d–e.** *A. crumena* individual number A4. **d.** Ventral view **e.** Dorsal view. **f.** Ventral view of *A. crumena* individual number A6 showing the 2‴ plate that has the round curve on the posterior part of the plate (asterisk). **g–i.** *A. crumena* individual number A7. **g.** Ventral view. **h.** Whole cell view showing two pusules (p) and the spines on the anterior part of the cell (arrowheads). **i.** Dorsal view showing the postcingular plates (4‴, 5‴) and antapical plates (1⁗, 2⁗). **j–m.** *A. crumena* individual number C3. **j.** Ventral view showing the spines on the anterior part of the cell (arrowheads). **k.** Ventral view showing the 2‴ plate that has the round curve (asterisk). **l.** Whole cell view showing two pusules (p) and the spines on the anterior part of the cell (arrowheads). **m.** Dorsal view showing nucleus (n). **n.** Dorsal view of *A. crumena* individual number C4 showing the third anterior intercalary plate 3a and the fourth postcingular plate (4‴). **o.** Dorsal epitheca of *A. crumena* individual number C5. **p.** Ventral view of *A. crumena* individual number C7 showing the pusule (p).

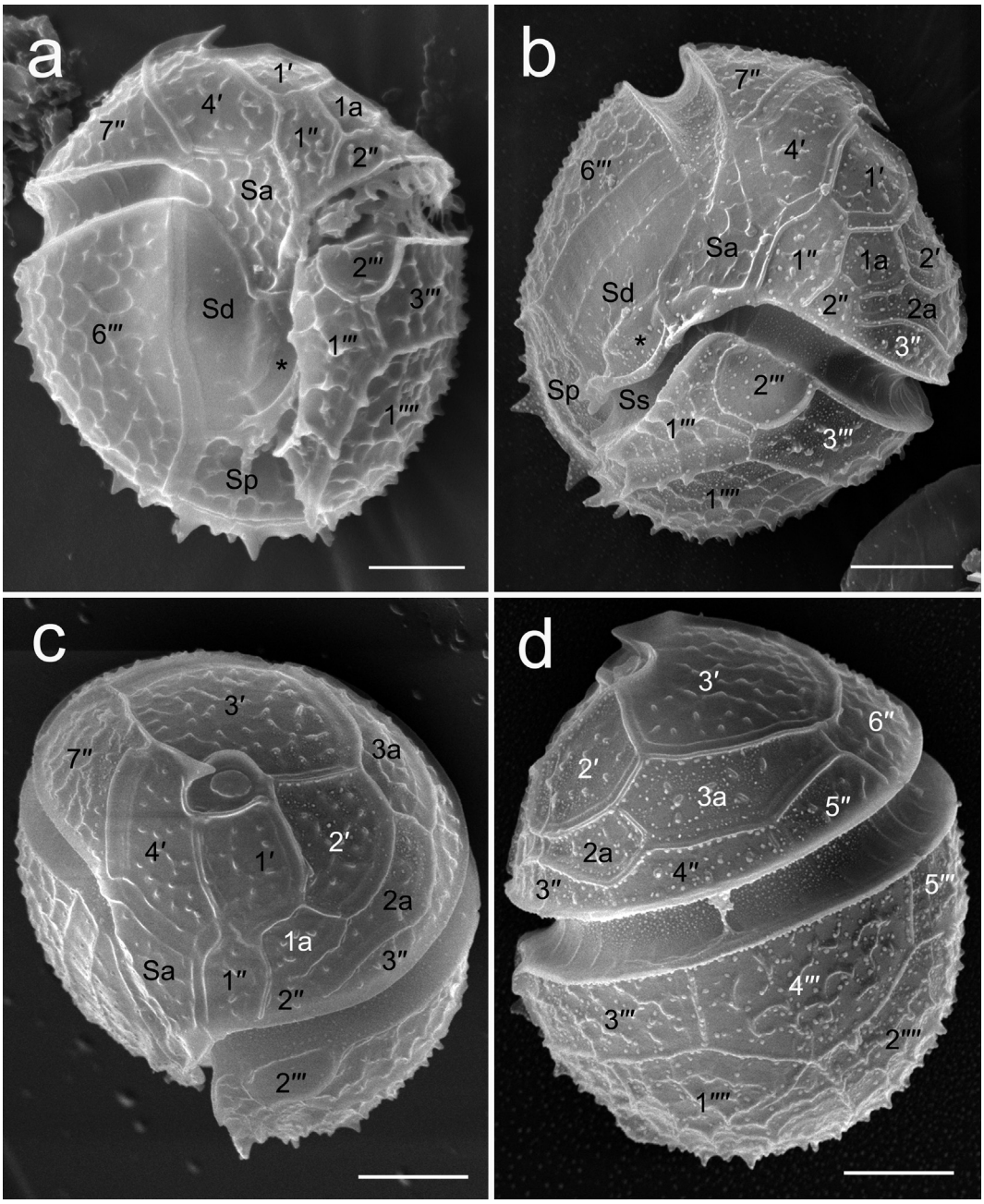

Fig. 2. SEM micrographs of *Amphidiniopsis crumena* from Kobe, Japan. Scabe bars = 5 µm. **a.** Holotype. Ventral view showing the apical plates (1′, 4′), the first anterior intercalary plate 1a, the precingular plates (1″, 2″, 7″), the anterior sulcal plate (Sa), the right sulcal plate (Sd), the wing of the Sd plate (asterisk), the posterior sulcal plate (Sp), the postcingular plates (1‴–3‴, 6‴), the first antapical plate (1⁗). **b.** Ventral view showing the apical plates (1′, 2′, 4′), the anterior intercalary plates 1a, 2a, the precingular plates (1″–3″, 7″), the anterior sulcal plate (Sa), the right sulcal plate (Sd), with characteristic wing (asterisk), the left sulcal plate (Ss), the posterior sulcal plate (Sp), the postcingular plates (1‴–3‴, 6‴), the first antapical plate (1⁗). **c.** Apical view showing the apical plates (1′–4′), the anterior intercalary plates (1a–3a), the precingular plates (1″–3″, 7″), the anterior sulcal plate (Sa), the second postcingular plates (2‴). **d.** Dorsal view showing the apical plates (2′, 3′), the anterior intercalary plate 2a, 3a, the precingular plates (3″–6″), the postcingular plates (3‴-5‴), the antapical plates (1⁗, 2⁗).

Thecal plates ornamented with protrusions (more or less spiny) on some plates as part of a mesh (reticulation), except for the smooth plate 2‴ and the cingular plates that are nearly smooth, only with faint transverse ribs (Figs. 2, 3). Some plate borders with marginal ridges, which are smooth on the epitheca but can also be spiny on the hypotheca. Scattered thecal pores (Fig. 3b, e). We did not find any information for the cyst stages.

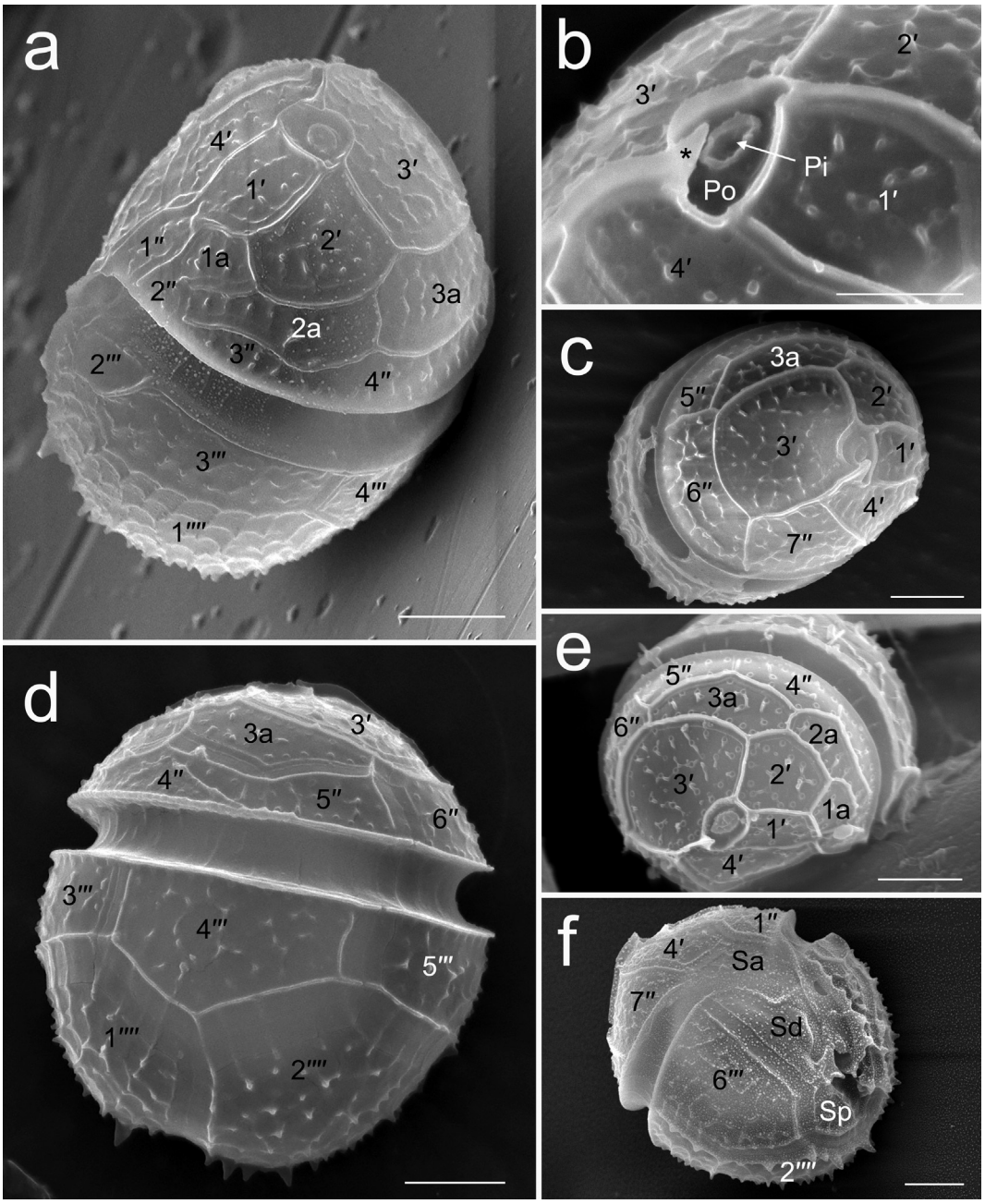

Fig. 3. SEM micrographs of *Amphidiniopsis crumena* from Kobe (**a–d**, **f**) and Okinawa (**e**), Japan. Scale bars = 5 μm (**a**, **c–f**) and 3 μm (**b**). **a.** Left lateral view showing the apical plates (1′–4′), the anterior intercalary plates (1a–3a), the precingular plates (1″–4″), the postcingular plates (2‴–4‴), the first antapical plate (1⁗). **b.** Apical view showing the apical plates (1′–4′) and the detail of the Apical Pore Complex (APC) including the cover plate (Pi) covering the apical pore, the pore plate (Po) surrounding the apical pore, the ridge of the fourth apical plate partly covering the APC (asterisk). **c.** Right apical view showing the apical plates (1′–4′), the third anterior intercalary plate 3a, the precingular plates (5″–7″). **d.** Dorsal view showing the third apical plate (3′), the third anterior intercalary plate 3a, the precingular plates (4″–6″), the postcingular plates (3‴–5‴), the antapical plates (1⁗, 2⁗). **e.** Apical view showing the apical plates (1′–4′), the anterior intercalary plates (1a–3a), the precingular plates (4″–6″). **f.** Right ventral view showing the fourth apical plate (4′), the precingular plates (1″, 7″), the anterior sulcal plate (Sa), the right sulcal plate (Sd), the posterior sulcal plate (Sp), the sixth postcingular plate (6‴), the second antapical plate (2⁗).

Molecular characterization: nuclear ribosomal 18S rRNA gene GenBank accessions LC333938–LC333942. 28S rRNA gene GenBank accessions LC340364–LC340372.

Holotype: Fixed and dried specimen on SEM stub (specimen shown in Fig. 2a), held in the Biodiversity Lab associated with the Hokkaido University Museum (SAP number: SAP115644).

Type locality: A tidal flat in Maiko, Kobe, Hyogo Prefecture (34°37′38.58″ N, 135°02′ 23.09″ E).

Distribution: Onna Village, Okinawa, Japan (26° 28′57.05″ N, 127°50′ 44.49″ E). Maiko, Hyogo, Japan (34°37′38.58″ N, 135°02′ 23.09″ E).

Habitat: marine, sand-dwelling, heterotroph.

Etymology: small money bag/pouch, *crumena* in Latin; the specific epithet refers to the unique shape, size and location of the second postcingular plate which reminds of a belt pouch.

Registration: http://phycobank.org/103417

Amphidiniopsis nileribanjensis Hoppenrath, Kretzschmar et Sh.Murray sp. nov.

Figs. 4, 5.

Description: Cells rounded in ventral view, dorsoventrally flattened, slightly longer than wide (Figs. 4, 5), 27.4–30.5 µm long (n = 6), and 25.0–27.7 µm wide (premedian) (n = 5). Apical hook pointing apically, slightly to the left cell side (Fig. 4c, d). No antapical spines (Fig. 4). No chloroplast, eyespot or recognizable food particles (Fig. 4). Pusules and nucleus not observed.

Thecal plate formula: APC 4′ 3a 7″ 3?C 4S 6‴ 2⁗ (Fig. 5). Apical Pore Complex (APC) with round to oval apical pore (Fig. 5h). First apical plate (1′) slightly shifted left laterally (Fig. 5a, b, g). Plate 2′ left lateral (Fig. 5d, h). Large plate 3′ located dorsally (Fig. 5e, f, h, j), likely forming the small apical hook (Fig. 5h). Fourth apical plate (4′) in ventral position (Fig. 5a, b, g, i). Small pentagonal plate 1a in left lateral position (Fig. 5b, d, g). Plate 2a is pentagonal and in left lateral position (Fig. 5d, g, h). Third anterior intercalary plate 3a hexagonal and wide, covering the left middle part of the dorsal epitheca (Fig. 5e, f, h, j). Wider first precingular plate (1″) than that of *A. crumena* (Fig. 5a, b, g, i). Very small plate 2″ (Fig. 5d, i). Long and narrow, pentagonal, plate 3″ in left lateral position (Fig. 5d, f, h, j). Fourth (4″) and fifth (5″) precingular plate relatively narrow, dorsal (Fig. 5f, h, j). Plate 6″ also narrow in right lateral position (Fig. 5c, f, h, j). Ventral seventh precingular plate (7″) pentagonal (Fig. 5b, c, g, i).

Cingulum wide, ascending, completely encircling the cell, composed of at least three plates (Fig. 5a, f, g, j). Wide sulcus consisting of non-recessed and recessed (forming the longitudinal furrow) plates. Non-recessed anterior sulcal plate (Sa) between right and left edge of the cingulum (Fig. 5a, b, g). Non-recessed, large right sulcal plate (Sd) with well-developed wing-like left list positioned mid ventral (Fig. 5a, b). Recessed, elongated left sulcal plate (Ss) connected to the left cingulum origin (Fig. 5b). Posterior sulcal plate (Sp) positioned antapically, longer left anterior side in contact with plate 1‴ (Fig. 5a). Serrated left sulcal list (Fig. 5a, c).

First postcingular plate (1‴) with irregular shape (Fig. 5a, b). Striking, plate 2‴ with unique pocket-like shape (Fig. 5a, b, d). Plate 4‴ symmetrical, pentagonal (Fig. 5e, f). Third (3‴) and fifth (5‴) postcingular plates in lateral position (Fig. 5c–f). Large plate 6‴ covering the right ventral hypotheca part (Fig. 5a–d). Two large antapical plates (1⁗ and 2⁗) are almost symmetrical on the dorsal hypothecal view (Fig. 5e, f).

Thecal plates ornamented with a more or less developed mesh (reticulation), except the nearly smooth plate 2‴ and the cingular plates, only with faint ribs/reticulations (Fig. 5). Some plate borders with marginal ridges. Scattered thecal pores as part of the mesh or as line along the postcingular plate borders (Fig. 5k). Very short postcingular list formed by the postcingular plates, except for plate 2‴ for which this list runs around the plate (formed by the connecting plates 1‴ and 3‴) (Fig. 5a, b, d). We did not find any information of cyst stage.

Molecular characterization: nuclear ribosomal 18S rRNA gene GenBank accession LC719582.

Holotype: Fig. 5a. The SEM stub was lost during laboratory relocation and thus only an image of the specimen is available as type material by following Division II, Chapter II, Section 2, Art. 9.1 in International Code of Nomencla-

Fig. 4. Light micrographs of *Amphidiniopsis nileribanjensis*. Scale bars = 10 µm. **a–c.** Same cell in different focal planes. **a.** Ventral view with focus on the cingulum ends. **b.** Slightly deeper focus on the left sulcal edge. **c.** Mid cell focus showing the apical hook (arrow). **d.** Mid cell focus, note the apical hook (arrow).

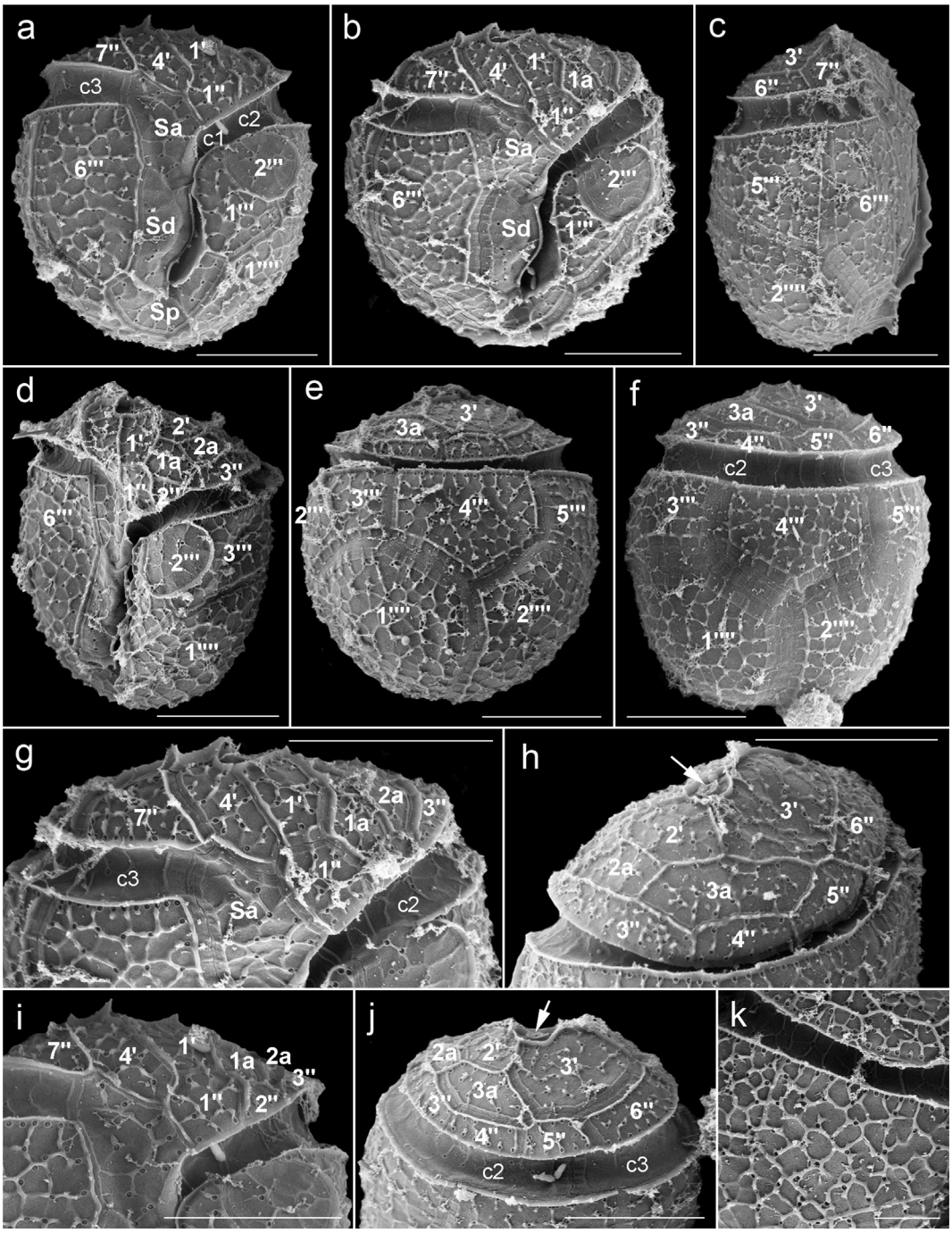

Fig. 5. SEM micrographs of *Amphidiniopsis nileribanjensis* showing the thecal tabulation and ornamentation. Scale bars = 10 μm, except in **k** 2 μm. **a**, **b.** Ventral view. Note the characteristic second postcingular plate (2‴). **c.** Right lateral view showing the cell flattening. **d.** Left lateral to ventral view. Note the characteristic second postcingular plate (2‴). **e**, **f.** Dorsal view. **g.** Ventral view of the epitheca. **h.** Left lateral to dorsal view of the epitheca showing the round to oval apical pore (arrow). Note that plate 3a is not contacting plate 6″. **i.** Ventral view of the epitheca. **j.** Dorsal view of the epitheca showing the round to oval apical pore (arrow). **k.** Detail of the thecal ornamentation.

ture for algae, fungi, and plants. It was from a field sample and no further fixed material is available.

Type locality: tidal flat of Cable Beach, Broome (17.9319° S, 122.2081° E).

Distribution: Cable and Town Beach, Broome, NW Australia.

Habitat: marine, sand-dwelling, heterotroph.

Fig. 6. Maximum-likelihood (ML) tree inferred from 18S rDNA sequences. ML bootstrap values over 80% and Bayesian posterior probabilities (PP) over 0.95 are shown at the nodes (ML/PP). Thick branches indicate maximal support (100/1.00). The scale bar represents inferred evolutionary distance in changes/site. The branches leading to the fast-evolving taxa are indicated by dashed and shortened by a quarter. The taxon names corresponding to DNA sequences generated in this study are indicated in bold and the box of grey gradation. Clade X is indicated by a grey box. The other clades are marked with vertical lines on the right and also dashed vertical lines.

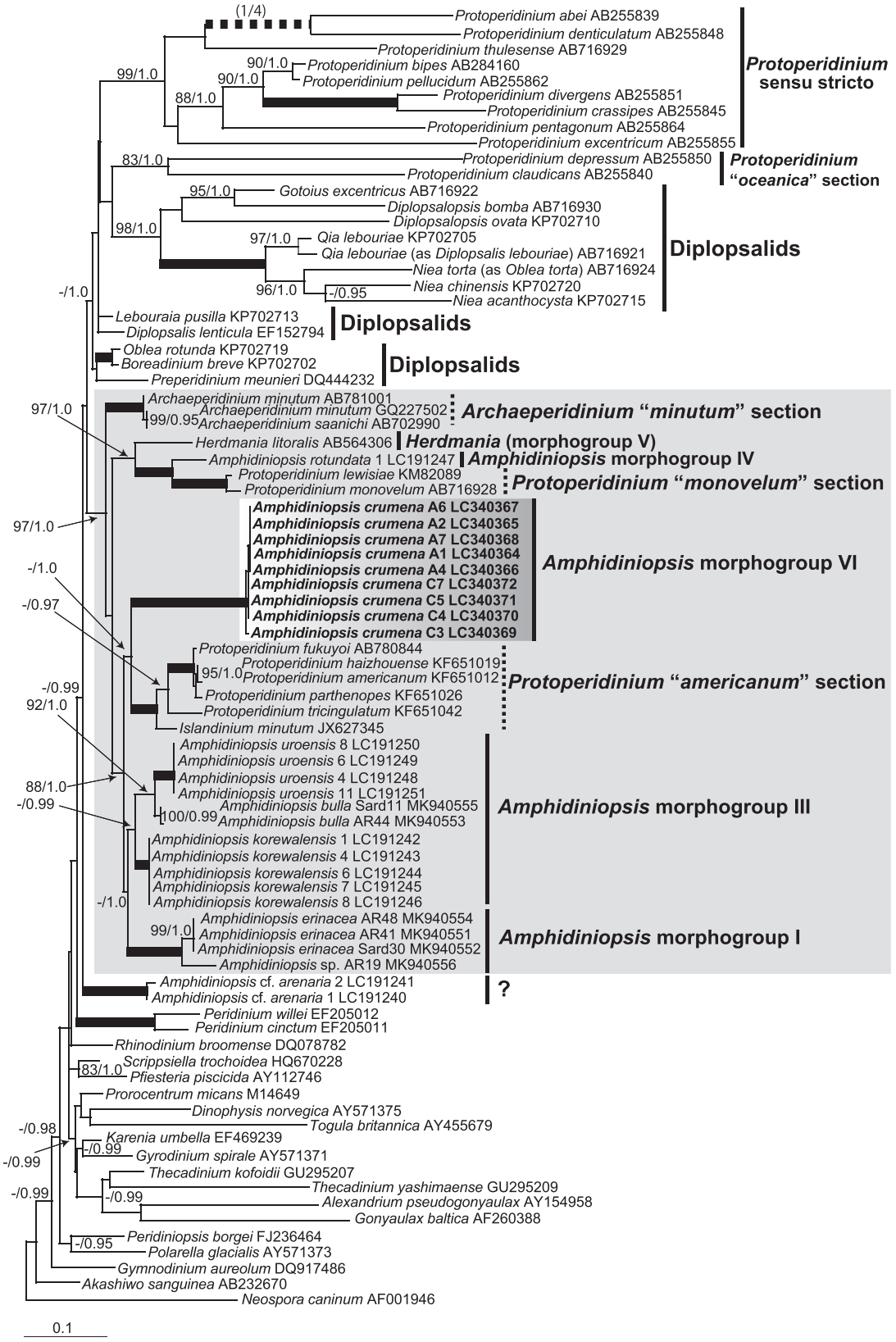

Fig. 7. Maximum-likelihood (ML) tree inferred from 28S rDNA sequences. Clade Y is indicated by a grey box. Other information is the same as Fig. 6.

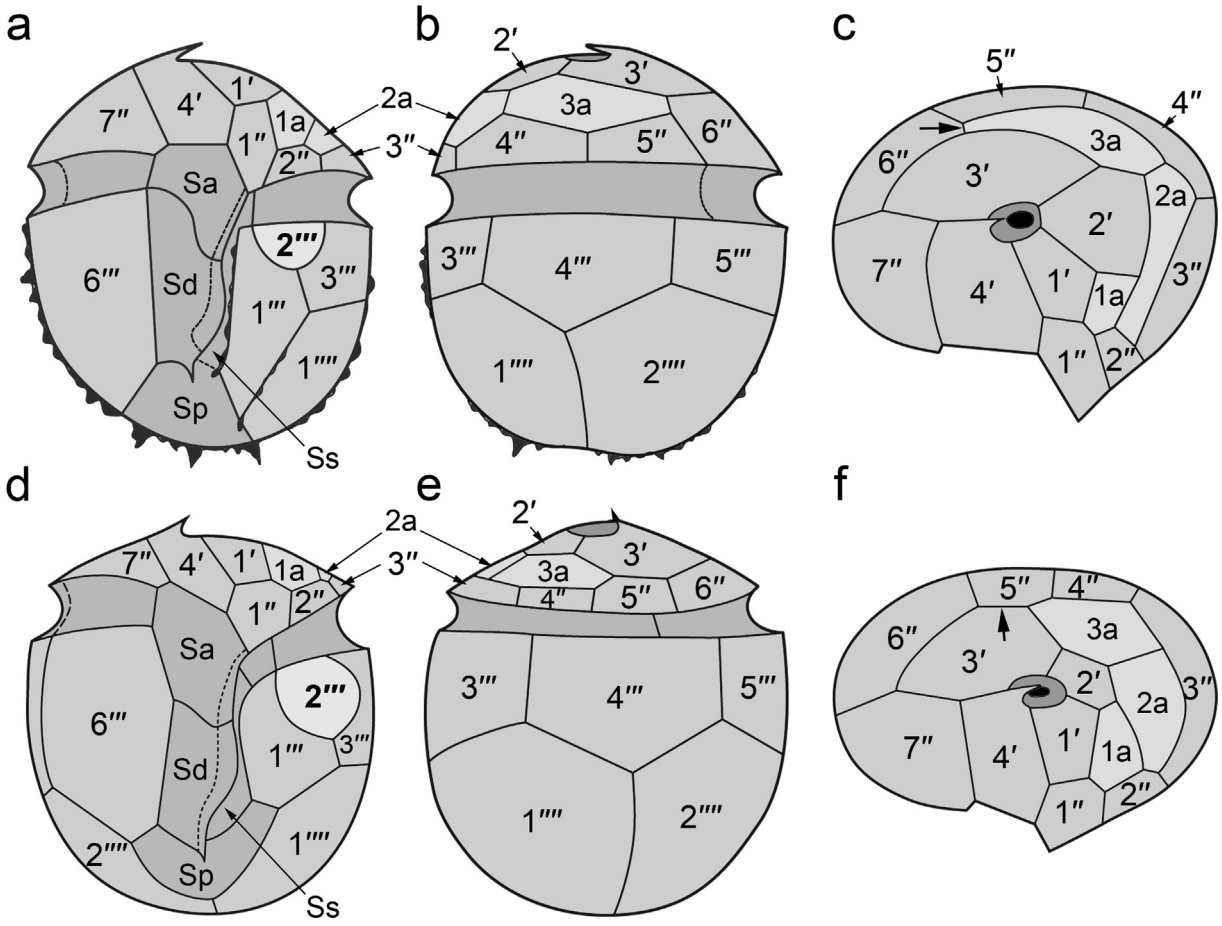

Fig. 8. Comparative line drawings of the thecal tabulation of *A. crumena* (a–c) and *A. nileribanjensis* (d–f). The two species are not drawn at scale. **a**, **d.** Ventral. **b**, **e.** Dorsal. **c**, **f.** Epitheca. Note the characteristic second postcingular plate and the specific differences of the anterior and right sulcal plates in (a) and (d). The epithecal tabulation (c, f) clearly differentiates the two species, especially the relative sizes, shapes, and locations of the anterior intercalary plates (1a–3a). Note that plate 3a is in contact with plate 6″ (arrow in (c)) in *A. crumena* but not in *A. nileribanjensis* where plates 3′ and 5″ are in contact (arrow in (f)).

Etymology: The name refers to the type locality Nileribanjen, which is an older name for Broome.

Registration: http://phycobank.org/103418

Phylogenetic analysis of 18S rDNA and 28S rDNA

For *Amphidiniopsis crumena*, the 18S rDNA sequences from 3 cells from Okinawa (A1, A6, A7) and 2 cells from Maiko (C3, C4) and one cell from Australia were generated (Fig. 6). Out of a total of 1757 base pairs (bp) that were compared, *A. crumena* C3 had 1 bp difference from the other sequences of this species (Fig. 6). The 28S rDNA sequences for *A. crumena* were amplified from 5 cells from Okinawa (A1, A2, A4, A6, A7) and 4 cells from Maiko (C3, C4, C5, C7) (Fig. 7). 1215 bp across the 28S rDNA were compared and there are three different sequences among 9 cells. The first group comprised all cells from Okinawa (A1, A2, A4, A6, A7). The second group were all cells from Maiko except for C3 (C4, C5, C7). Among the sequences of 9 cells, *A. crumena* C3 was the most different from the sequences of other cells. It differed 12 bp with the first (A1, A2, A4, A6, A7) and second group (C4, C5, C7), respectively. The first and second groups differed in 4 bp each other.

In the 18S rDNA analyses, *A. crumena* and *A. nileribanjensis* formed a clade with 100% ML bootstrap support and 1.0 Bayesian PP. This clade is positioned in the highly supported (98% ML bootstrap support/1.0 Bayesian PP) Clade X, which is indicated in a gray box on Fig. 6, comprises ten *Amphidiniopsis* species (*A. bulla*, *A. dragescoi*, *A. elongata*, *A. erinacea*, *A. hexagona*, *Amphidiniopsis* cf. *kofoidii*, *A. korewalensis*, *A. rotundata*, *Amphidiniopsis* sp. AR19, *A. uroensis*), five species of the *Protoperidinium* "*americanum*" section in Protoperidiniaceae, *Protoperidinium monovelum* (*Protoperidinium* "*monovelum*" section), *Herdmania litoralis* and two species of *Archaeperidinium* (*Archaeperidinium* "*minutum*" section) (Fig. 6). In Clade X, *A. crumena* and *A. nileribanjensis*

formed a subclade with *Protoperidinium* "*americanum*" section, *Amphidiniopsis* morphogroup I (*A. erinacea*, *Amphidiniopsis* cf. *kofoidii*, *Amphidiniopsis* sp. AR19) and *Amphidiniopsis* morphogroup III (*A. bulla*, *A. elongata*, *A. kolewalensis*, *A. uroensis*) with 95% ML bootstrap support and 1.0 Bayesian PP and take the most basal position. In 28S rDNA analyses, *A. crumena* positioned in Clade Y, which is indicated in a gray box on Fig. 7, that is formed by six *Amphidiniopsis* species (*A. bulla*, *A. erinacea*, *A. korewalensis*, *A. rotundata*, *Amphidiniopsis* sp. AR19, *A. uroensis*), six species of *Protoperidinium* "*americanum*" section, two species of *Protoperidinium* "*monovelum*" section, *Herdmania litoralis* and two species of *Archaeperidinium* "*minutum*" section with high statistical support (97% ML bootstrap support/1.0 Bayesian PP) (Fig. 7). In Clade Y, *A. crumena* formed a clade with *Protoperidinium* "*americanum*" section, *Amphidiniopsis* morphogroup I (*A. erinacea*, *Amphidiniopsis* sp. AR19) and *Amphidiniopsis* morphogroup III (*A. bulla*, *A. kolewalensis*, *A. uroensis*) with 88% ML bootstrap support and 1.0 Bayesian PP. The closest relative of *Amphidiniopsis* morphogroup VI is *Protoperidinium* "*americanum*" section (–/1.0) (Fig. 7).

Discussion

In this study, we have identified two new species of the peridinioid, benthic sand-dwelling heterotrophic dinoflagellate genus, *Amphidiniopsis*. We found that the species *Amphidiniopsis crumena* could be distinguished from *A. nileribanjensis* as it possesses several spines on the hypotheca. Plate 1″ in *A. crumena* is narrower than plate 1″ in *A. nileribanjensis* (Figs. 2a, 5a, b, g, i, 8). The second anterior intercalary plate 2a is in contact with the fourth precingular plate in *A. crumena* but not in *A. nileribanjensis* (Figs. 2d, 3a, e, 5h, j, 8). The third anterior intercalary plate 3a is in a mid-dorsal position and in contact with the sixth precingular plate (6″) in *A. crumena* but not in *A. nileribanjensis* (left-dorsal position) (Figs. 2d, 5h). This implies that plate 3′ contacts 5″ in *A. nileribanjensis* but not in *A. crumena* (Figs. 2d, 3c–e, 5e–f, h, j, 8). The shape of plate 1‴ of *A. crumena* is elongated but relatively shorter and wider for *A. nileribanjensis* (Figs. 2a, b, 5a, b, 8). The second postcingular plate (2‴) from *A. crumena* has a belt pocket-like shape, but is comparatively more rounded and forms a nearly complete circle for *A. nileribanjensis* (Figs. 2a, b, 5a, b, d, 8). The anterior sulcal plate (Sa) in *A. nileribanjensis* touches with the sixth postcingular plate (6‴) but not in *A. crumena* (Figs. 2a, b, 5a, b, 8).

The two new species are members of the genus *Amphidiniopsis* due to their smaller epitheca and a larger hypotheca, an ascending cingulum, and a distinctive curved sulcus (Hoppenrath et al. 2014). Except for *Amphidiniopsis dragescoi* (Balech) Hoppenrath, Selina, Yamaguchi et Leander, all species in the genus *Amphidiniopsis* have the typical hypothecal plate pattern, which has five postcingular plates and two antapical plates (Hoppenrath et al. 2014; Reñé et al. 2020; Selina and Morozova 2016). *Amphidiniopsis dragescoi* has only four postcingular plates and a descending cingulum and its affiliation to *Amphidiniopsis* morphogroup IV is problematic (Hoppenrath et al. 2014; Reñé et al. 2020). Both new species, *A. crumena* and *A. nileribanjensis*, have six postcingular plates and two antapical plates. Possessing six postcingular plates is the unique feature of the two new species. In most species of *Amphidiniopsis*, plate 3‴ covers the large part of the dorsal hypotheca. In these two new species, plate 4‴ is located in that dorsal hypotheca position and it looks homologous with plate 3‴ of other *Amphidiniopsis* species. The second postcingular plate (2‴) is unique to these two new species and looks like an additional plate that 'appeared' between plates 1‴ and 3‴ on the edge of the cingulum. It appears as though parts of two homologous plates generally present in *Amphidiniopsis* species (1‴ and 2‴) were separated and fused in these two new species of *Amphidiniopsis*. Its special shape, being rounded (not polygonal) and its curved outline is characteristic and even noticeable by light microscopy (Fig. 1). An unusual rounded plate with loop-shape was described in *Amphidiniopsis bulla* Reñé, Satta et Hoppenrath and *A. cristata* Hoppenrath (Hoppenrath 2000; Reñé et al. 2020) but in a different thecal position. That second precingular plate (2″) is smooth, without pores (Hoppenrath 2000; Reñé et al. 2020). Reñé et al. (2020) mentioned that *A. bulla* and *A. cristata* belong to the *Amphidiniopsis* morphogroup III ('*uroensis* group') that includes dorsoventrally flattened species with the sulcus only slightly (or not) displaced, and an apical hook. This group includes *A. korewalensis*, *A. uroensis*, *A. pectinaria*, *A. hoppenrathae*, *A. elongata*, *A. bulla* and *A. cristata*. Reñé et al. (2020) also suggested the possibility that *A. bulla* and *A. cristata* will be separated as the *Amphidiniopsis* morphogroup IIIa ('*cristata* group'), based on the morphologically unique feature of this loop-shaped second precingular plate (2″). However, the molecular phylogenetic data from *A. cristata* are not available, so this separation is only tentative. *Amphidiniopsis crumena* and *A. nileribanjensis* have an unusual second postcingular plate (2‴) reminding of a belt pouch, a feature suitable for morphogroup characterization.

The curved line of plate 2‴ is reminiscent the experiments by Sekida et al. (2012). This work showed that the thecal plate variations appeared when the cells of the thecate dinoflagellate *Scrippsiella hexapraecingula* Horiguchi et Chihara were experimentally treated in a high-pressure environment (in a high-pressure chamber). The variations in the thecal plate pattern shown in Sekida et al. (2012) included plates with curved suture, fusion of the part of plates, insertion of the small plates or small and round plates. They mentioned that these variations were caused by the disorganized cortical microtubules, under high pressure, leading to a change in the thecal plate pattern (Sekida

et al. 2012). It does not seem likely that high-pressure was the cause of this variation in *A. crumena* and *A. nileribanjensis* because high-pressure has not been shown to permanently change the morphology of subsequent dinoflagellate generations. However, it might be possible that the unique 2‴ plate of *A. crumena* and *A. nileribanjensis* has been influenced by unusual cortical microtubular patterns caused by some sort of genetical event in their ancestor lineage as one evolutionary event, followed by distribution of the lineage and further speciation in widely geographically separated regions (Australia and Japan).

Previous molecular phylogenetic studies showed that most *Amphidiniopsis* species (with the exception of *Amphidiniopsis* cf. *arenaria*) were related to the family Protoperidiniaceae (Reñé et al. 2020; Yamaguchi et al. 2016). Most *Amphidiniopsis* species with genetic information available cluster with *Herdmania litoralis*, *Archaeperidinium* species, and the species of the *Protoperidinium* "*monovelum*" and "*americanum*" sections (Figs. 6, 7; Yamaguchi et al. 2011, 2016). In the family Protoperidiniaceae, it is common to have the five postcingular plates and two hypothecal plates, except for the diplopsalids which have five postcingular and one or two antapical plates (Liu et al. 2015). Among the species of the family Protoperidiniaceae and the genus *Amphidiniopsis*, the number of postcingular plates is stable, except for *A. crumena* and *A. nileribanjensis* (and *A. dragescoi* as previously mentioned). Because of the unique 2‴ plate and the six postcingular plates, *A. crumena* and *A. nileribanjensis* are suitable to be assigned to a new morphogroup.

Through the 18S rDNA and 28S rDNA phylogenetic analyses, Reñé et al. (2020) confirmed that the species of *Amphidiniopsis* were not monophyletic and that at least four phylogenetic subgroups existed. They also newly termed *Amphidiniopsis* as a genus complex and included the monotypic genus *Herdmania* because its morphological characters had similarity with the other *Amphidinopsis* species. So far, the *Amphidiniopsis* genus complex contains at least five morphogroups; these morphogroups coincided with their molecular phylogenetic positions (*Amphidiniopsis* morphogroup I '*kofoidii* group', morphogroup II '*hirsuta* group', morphogroup III '*uroensis* group', morphogroup IV '*rotundata* group' and morphogroup V '*Herdmania* group') (Reñé et al. 2020). It is also mentioned that *A. cristata* and *A. bulla* would be separated from morphogroup III into the morphogroup IIIa '*cristata* group' when the molecular phylogenetic data of *A. cristata* will be available and supportive for these two species.

It is concluded that the here presented two new species formed a clade and did not belong to any of the described morphogroups. Therefore, a further new morphogroup, *Amphidiniopsis* morphogroup VI '*crumena* group' is proposed. The two new species have a dorsoventrally flattened cell shape, an apical hook, a complete cingulum, a slightly displaced (or not displaced) sulcus, six postcingular plates and a curved belt pocket-like, and a roundish second postcingular plate.

In the present 18S rDNA phylogeny (Fig. 6), the *Amphidiniopsis* morphogroup IV did not form a monophyletic clade. *Amphidiniopsis dragescoi* (morphogroup IV) was positioned at the base of the clade comprised of *Herdmania litoralis* (morphogroup V), *Protoperidinium monovelum* (*Protoperidinium* "*monovelum*" section) and *Amphidiniopsis rotundata* (morphogroup IV). As mentioned above, *A. dragescoi* is a controversial species and its affiliation to morphogroup IV is problematic because it possesses only four postcingular plates and a descending cingulum (Hoppenrath et al. 2014; Reñé et al. 2020).

Three sections in the family Protoperidiniaceae i.e. *Protoperidinium* "*monovelum*" section, *Protoperidinium* "*americanum*" section, *Archaeperidinium* "*minutum*" section, and *Amphidiniopsis* morphogroups I-VI formed a clade with high support (98/1.00) (Fig. 6). This is equivalent to Clade X in previous studies (Reñé et al. 2020; Yamaguchi et al. 2011). The 28S rDNA phylogeny also showed a highly supported clade comprised of three sections in the family Protoperidiniaceae and *Amphidiniopsis* morphogroups I, III, IV, V and VI (molecular phylogenetic data of *Amphidiniopsis* morphogroup II were not available). This clade was called Clade Y in the previous studies (Reñé et al. 2020; Yamaguchi et al. 2011).

Since our new species are categorized as a new morphogroup, *Amphidiniopsis* morphogroup VI, there are now seven morphogroups (including *Amphidiniopsis* morphogroup IIIa) in total that are supposed to position in Clade X for 18S rDNA analysis and in Clade Y for 28S rDNA analysis (as mentioned before, the molecular phylogenetic data of morphogroup II is not available for 28S rDNA) within the *Amphidiniopsis* genus complex. The accumulation of knowledge of the morphological features and their molecular phylogenetic relationships for these taxa is necessary for further taxonomic conclusions and a revision of the systematics.

Data availability

Data will be made available on request.

Acknowledgments

This work was supported by JSPS KAKENHI Grant Numbers 17K15173 and 21J40057 to AY and 18K14774 to KCW. Financial support to conduct the sampling in Broome, Western Australia (SM and MH) was provided by the Australian Biological Resources Study Grant RFL210-34. SM thanks the Hanse-Wissenschaftskolleg, Delmenhorst, Germany for fellowship support. We thank Nicolas Chomérat for help in finding a species name and Gurjeet Kohli for assistance with sample collection.

References

Castresana, J., 2000. Selection of conserved blocks from multiple alignments for their use in phylogenetic analysis. Mol. Biol. Evol. 17, 540–552. https://doi.org/10.1093/oxfordjournals.molbev.a026334.

Dodge, J.D., Lewis, J., 1986. A further SEM study of armoured sand-dwelling marine dinoflagellates. Protistologica 22, 221–230.

Edgar, R.C., 2004. MUSCLE: multiple sequence alignment with high accuracy and high throughput. Nucleic Acids Res. 32, 1792–1797.

Fensome, R.A., Taylor, F.J.R., Norris, G., Sarjeant, W.A.S., Wharton, D.I., Williams, G.L., 1993. A classification of living and fossil dinoflagellates. USA: Sheridan (PA).

Gómez, F., López-García, P., Moreira, D., 2011. Molecular phylogeny of the sand-dwelling dinoflagellates *Amphidiniopsis hirsuta* and *A. swedmarkii* (Peridiniales, Dinophyceae). Acta Protozool. 50, 255–262.

Hoppenrath, M., 2000. Morphology and taxonomy of six marine sand-dwelling *Amphidiniopsis* species (Dinophyceae, Peridiniales), four of them new, from the German Bight, North Sea. Phycologia, 482–497.

Hoppenrath, M., Murray, S., Chomérat, N., Horiguchi, T., 2014. Marine benthic dinoflagellates - unveiling their worldwide biodiversity. Kleine Senckenberg-Reihe 54. Senckenberg Gesellschaft für Naturforschung, Senckenberganlage 25 Frankfurt am Main, Germany.

Hoppenrath, M., Koeman, R.P.T., Leander, B.S., 2009. Morphology and taxonomy of a new marine sand-dwelling *Amphidiniopsis* species (Dinophyceae, Peridiniales), *A. aculeata* sp. nov., from Cap Feret, France. Mar. Biodivers. 39, 1–7.

Hoppenrath, M., Selina, M., Yamaguchi, A., Leander, B.S., 2012. Morphology and molecular phylogeny of *Amphidiniopsis rotundata* sp. nov. (Peridiniales, Dinophyceae), a benthic marine dinoflagellate. Phycologia 51, 157–167.

Horiguchi, T., Yoshizawa-Ebata, J., Nakayama, T., 2000. *Halostylodinium arenarium*, gen. et sp. nov. (Dinophyceae), a coccoid sand-dwelling dinoflagellate from subtropical Japan. J. Phycol. 36, 960–971.

Litaker, W., Steidinger, K.A., Mason, P.L., Landsberg, J.H., Shields, J.D., Reece, K.S., Haas, L.W., Vogelbein, W.K., Vandersea, M.W., Kibler, S.R., Tester, P.A., 2005. The reclassification of *Pfiesteria shumwayae* (Dinophyceae): *Pseudopfiesteri*a, gen. nov. J. Phycol. 41, 643–651.

Liu, T., Mertens, K.N., Gu, H., 2015. Cyst–theca relationship and phylogenetic positions of the diplopsalioideans (Peridiniales, Dinophyceae), with description of *Niea* and *Qia* gen. nov.. Phycologia 54, 210–232.

Maddison, W.P., Maddison, D.R., 2015. Mesquite: a modular system for evolutionary analysis. Version 3, 03 http://mesquiteproject.org.

Murray, S., Patterson, D.J., 2002. *Amphidiniopsis korewalensis* sp. nov., a new heterotrophic benthic dinoflagellate. Phycologia 41, 382–388.

Nishimura, T., Sato, S., Tawong, W., Sakanari, H., Uehara, K., Shah, M.M.R., Suda, S., Yasumoto, T., Taira, Y., Yamaguchi, H., Adachi, M., 2013. Genetic diversity and distribution of the ciguatera-causing dinoflagellate *Gambierdiscus* spp. (Dinophyceae) in coastal areas of Japan. PLoS ONE 8, e60882.

Nunn, G.B., Theisen, B.F., Christensen, B., Arctander, P., 1996. Simplicity-correlated size growth of the nuclear 28S ribosomal RNA D3 expansion segment in the crustacean order Isopoda. J. Mol. Evol. 42, 211–223.

Reñé, A., Satta, C.T., López-García, P., Hoppenrath, M., 2020. Re-evaluation of *Amphidiniopsis* (Dinophyceae) morphogroups based on phylogenetic relationships, and description of three new sand-dwelling species from the NW Mediterranean. J. Phycol. 56, 68–84.

Ronquist, F., Huelsenbeck, J.P., 2003. MRBAYES 3: Bayesian phylogenetic inference under mixed models. Bioinformatics 19, 1572–1574.

Scholin, C.A., Herzog, M., Sogin, M., Anderson, D.M., 1994. Identification of group- and strain-specific genetic markers for globally distributed *Alexandrium* (Dinophyceae). II. Sequence analysis of a fragment of the LSU rRNA gene. J. Phycol. 30, 999–1011.

Sekida, S., Takahara, M., Horiguchi, T., Okuda, K., 2012. Effects of high pressure in the armored dinoflagellate *Scrippsiella hexapraecingula* (Peridiniales, Dinophyceae): changes in thecal plate pattern and microtubule assembly. J. Phycol. 48, 163–173.

Selina, M.S., Hoppenrath, M., 2013. Morphology and taxonomy of seven marine sand-dwelling *Amphidiniopsis* species (Peridiniales, Dinophyceae), including two new species, *A. konovalovae* sp. nov. and *A. striata* sp. nov., from the Sea of Japan. Russia. Mar. Biodivers. 43, 87–104.

Selina, M.S., Morozova, T.V., 2016. Morphology and taxonomy of three new marine sand-dwelling *Amphidiniopsis* species (Peridiniales, Dinophyceae) from the Sea of Japan, Russia. Phycologia 56, 1–13.

Takano, Y., Horiguchi, T., 2004. Surface ultrastructure and molecular phylogenetics of four unarmoured heterotrophic dinoflagellates, including the type species of the genus *Gyrodinium* (Dinophyceae). Phycol. Res. 52, 107–116.

Talavera, G., Castresana, J., 2007. Improvement of phylogenies after removing divergent and ambiguously aligned blocks from protein sequence alignments. Syst. Biol. 56, 564–577.

Toriumi, S., Yoshimatsu, S., Dodge, J.D., 2002. *Amphidiniopsis uroensis* sp. nov. and *Amphidiniopsis pectinaria* sp. nov. (Dinophyceae): two new benthic dinoflagellates from Japan. Phycol. Res. 50, 115–124.

Trifinopoulos, J., Nguyen, L.T., von Haeseler, A., Minh, B.Q., 2016. W-IQ-TREE: a fast online phylogenetic tool for maximum likelihood analysis. Nucleic Acids Res. 44, W232–W235.

Uhlig, G., 1964. Eine einfache methode zur extraktion der vagilen, mesopsammalen microfauna. Helgol. Wiss. Meeresunters. 11, 178–185.

Wołoszy ska, J., 1928. Dinoflagellate der polnischen Ostsee swie der an Piasnica gelegenen Sümpfe. Archives d'Hydrobiologie et d'Ichtyologie 3, 153–278.

Yamaguchi, A., Kawamura, H., Horiguchi, T., 2006. A further phylogenetic study of the heterotrophic dinoflagellate genus, *Protoperidinium* (Dinophyceae) based on small and large subunit ribosomal RNA gene sequences. Phycol. Res. 54, 317–329.

Yamaguchi, A., Hoppenrath, M., Pospelova, V., Horiguchi, T., Leander, B.S., 2011. Molecular phylogeny of the marine sand-dwelling dinoflagellate *Herdmania litoralis* and an emended description of the closely related planktonic genus *Archaeperidinium* Jörgensen. Eur. J. Phycol. 46, 98–112.

Yamaguchi, A., Yoshimatsu, S., Hoppenrath, M., Wakeman, K. C., Kawai, H., 2016. Molecular phylogeny of the benthic dinoflagellate genus *Amphidiniopsis* and its relationships with the family Protoperidiniaceae. Protist 167, 568–583.

Yoshimatsu, S., Toriumi, S., Dodge, J.D., 2000. Light and scanning microscopy of two benthic species of *Amphidiniopsis* (Dinophyceae), *Amphidiniopsis hexagona* sp. nov. and *Amphidiniopsis swedmarkii* from Japan. Phycol. Res. 48, 107–113.

Zhang, H., Bhattacharya, D., Lin, S., 2005. Phylogeny of dinoflagellates based on mitochondrial cytochrome b andnuclear small subunit rDNA sequence comparisons. J. Phycol. 41, 411–420.